Insights into the DNA repair process by the formamidopyrimidine-DNA glycosylase investigated by molecular dynamics

PATRICIA AMARA,[1] LAURENCE SERRE,[2] BERTRAND CASTAING,[3] AND ALINE THOMAS[1]

[1]Laboratoire de Dynamique Moléculaire and [2]Laboratoire des Protéines Membranaires, Institut de Biologie Structurale Jean-Pierre Ebel Commissariat à l'énergie Atomique (CEA)/Centre National de la Recherche Scientifique (CNRS)/Université Joseph Fourier (UJF), 38027 Grenoble Cedex 1, France
[3]Centre de Biophysique Moléculaire Unité Propre de Recherche 4301, Centre National de la Recherche Scientifique (CNRS), 45071 Orléans Cedex 02, France.

(RECEIVED March 29, 2004; FINAL REVISION May 18, 2004; ACCEPTED May 18, 2004)

Abstract

Formamidopyrimidine-DNA glycosylase (Fpg) identifies and removes 8-oxoguanine from DNA. All of the X-ray structures of Fpg complexed to an abasic site containing DNA exhibit a common disordered region present in the C-terminal domain of the enzyme. However, this region is believed to be involved in the damaged base binding site when the initial protein/DNA complex is formed. The dynamic behavior of the disordered polypeptide (named Loop) in relation to the supposed scenario for the DNA repair mechanism was investigated by molecular dynamics on different models, derived from the X-ray structure of *Lactococcus lactis* Fpg bound to an abasic site analog-containing DNA and of *Bacillus stearothermophilus* Fpg bound to 8-oxoG. This study shows that the presence of the damaged base influences the dynamics of the whole enzyme and that the Loop location is dependent on the presence and on the conformation of the 8-oxoG in its binding site. In addition, from our results, the conformation of the 8-oxoG seems to be favored in *syn* in the *L. lactis* models, in agreement with the available X-ray structure from *B. stearothermophilus* Fpg and with a possible catalytic role of the flexibility of the Loop region.

Keywords: molecular dynamics; DNA repair; 8-oxoguanine; Fpg

Reactive oxygen species induce DNA lesions that may interfere with DNA replication fidelity and efficiency. To avoid the deleterious effects of these DNA damages, prokaryote and eukaryote organisms have developed enzymatic tools to repair DNA and eliminate the damaged nucleotides from the genome (Lindahl 1993). In bacteria, the formamido-pyrimidine DNA glycosylase (Fpg or MutM) was characterized for its ability to excise the imidazole ring-opened purines (Fapy nucleotides; Chetsanga and Lindahl 1979) and a wide range of oxidized bases such as 7, 8-dihydro-8-oxoG; (Tchou et al. 1991; Duarte et al. 2000). Fpg is a bifunctional glycosylase enzyme that excises the damaged base via the nucleophilic attack of C_1' by the amino group of Pro 1, leading to the cleavage of the N_9-C_1' bond (glycosylase activity) and the successive cuts of the 3′ and 5′ phosphodiester bonds of the abasic site (so-called AP-lyase activity; O'Connor and Laval 1989).

The crystal structure of DNA-free *Thermus thermophilus* Fpg (Sugahara et al. 2000) showed that Fpg is made of two major domains: the N-terminal and the C-terminal domains, the latter being subdivided into two DNA binding motifs: the H2TH and the zinc finger subdomains. The conserved

Reprint requests to: Patricia Amara or Laurence Serre, Institut de Biologie Structurale Jean-Pierre Ebel CEA/CNRS/UJF, 41 rue Jules Horowitz, 38027 Grenoble Cedex 1, France; e-mail: amara@ibs.fr or serre@ibs.fr; fax: 33-4-38785494.

Abbreviations: AP, apuric; 8-oxoG, 8-oxoguanine; *L. lactis*, X-ray structure of Fpg from *Lactococcus lactis* bound to an abasic site analog-containing DNA; Loop, residues 217–225 in *L. lactis* and corresponding residues in other Fpgs; freein, freeout, oxosynin, oxosynout, and oxoantiin, theoretical models derived from *L. lactis* with different conformations of the Loop, orienting Tyr 222 inside ("in") or outside ("out") the cavity, free or 8-oxoG-bound in *syn* or *anti*; *B. stearothermophilus*, X-ray structure of Fpg from *Bacillus stearothermophilus* bound to an 8-oxoG-containing DNA; bsoxo, theoretical model derived from *B. stearothermophilus*; *T. thermophilus*, X-ray structure of Fpg from *Thermus thermophilus*; MD, molecular dynamics; rmsd, root mean square deviation.

Article and publication are at http://www.proteinscience.org/cgi/doi/10.1110/ps.04772404.

sequence PELPEVET containing the catalytic Pro 1 is sandwiched between both major domains. This first structural work was followed by the structure determinations of several Fpg/abasic site-containing oligonucleotide complexes that gave important insights into the damaged DNA recognition by Fpgs: *Lactococcus lactis* Fpg P1G mutant complexed to a 1,3-propanediol abasic site analog-containing DNA (Serre et al. 2002), *Escherichia coli* Fpg covalently cross-linked to an AP site (Gilboa et al. 2002), *Bacillus stearothermophilus* Fpgs complexed with different AP sites and the end reaction product (Fromme and Verdine 2002). These structures show that each domain plays the role of a half-pinch retaining and bending the DNA. The damaged base is bound under an extra helical conformation. In all Fpg structures, the damaged base lies in a region delimitated by four segments, namely, 1–5, 74–78, 172–173, and 217–224 (numbering of the *L. lactis* enzyme). However, all of these DNA/enzyme models led to few data on the 8-oxoG recognition except that a loop present in the C-terminal domain could be part of the damaged base binding site (Fromme and Verdine 2002; Gilboa et al. 2002; Serre et al. 2002). We call the "Loop" the region 217–225 in *L. lactis* and corresponding residues in other Fpg models. The Loop is included in the large nonregularly folded zone 214–250 that joins the α-helix F and the β-strand number 9. Surprisingly, the primary sequence of the Loop is not much conserved in the Fpg family (see Table 1) and part of its structure is disordered in the crystal models obtained with AP sites and different sources of Fpg (residues 220 to 223 missing in *L. lactis*, as well as residues 217 to 224 in *E. coli*). The damaged base binding site seems large enough to accommodate the 8-oxoG under the *syn* or *anti* conformation (Serre et al. 2002). Recently, the structure of a glycosylase-deficient mutant E3Q of the *B. stearothermophilus* Fpg complexed to an 8-oxoG containing DNA (Fromme and Verdine 2003) showed that the 8-oxoG binds in the *syn* conformation, interacting strongly with a well-ordered Loop (220_{bs}-228_{bs}). The equivalent Loop is also completely defined in the DNA-free Fpg from *T. thermophilus* and has a conformation close to the one described in the complex between *B. stearothermophilus* Fpg and the 8-oxoG. Meanwhile, Zaika and coworkers (2003) constructed a model for the Loop and the 8-oxoG in the *E. coli* enzyme and analyzed it with MD simulations. Their results prompted them to favor the *anti* conformation of the 8-oxoG, in contradiction with the X-ray data of *B. stearothermophilus* Fpg. They explained this discrepancy by the fact that the *B. stearothermophilus* Fpg is an inactive mutant and proposed that this *syn* conformation might not result from a true specificity but from a statistically probable feature.

The movement of the Loop is believed to be related to different steps of the reaction, that is: (1) recognition of the oxidized base, (2) glycosylase reaction, and (3) βδ-elimination of the resulting abasic site (Fromme and Verdine 2003). To understand if this movement is meaningful and is required by the catalytic scenario, we employed theoretical methods to investigate the dynamic behavior of the Loop in the presence or the absence of the 8-oxoG. MD simulations (Karplus 2003) were performed on different models of the *L. lactis* enzyme (Serre et al. 2002) complexed either to an AP site (the 1,3 propanediol seen in the crystal) or to an 8-oxoG containing DNA (*syn* or *anti*), and with two starting conformations for the missing part of the Loop (220–223), differing in the orientation of Tyr 222 toward the protein interior or the solvent. We also present MD results obtained with the *B. stearothermophilus* Fpg complexed to an 8-oxoG containing DNA (Fromme and Verdine 2003) for comparison. The interaction of the Loop with the 8-oxoG binding site and with the damaged base, the correlation between the Loop motion and its conformation, the absence or presence of the 8-oxoG, and the movement of the whole enzyme were analyzed to assign a possible role of this Loop in DNA lesion recognition and excision.

Results

Validity of the models

For each model (see Materials and Methods for their definitions), we compared the experimental and theoretically derived B-factors. Despite the shift in the absolute values, probably due to crystal disorder not included in our calculations, the structural features are well reproduced in the theoretical models related to *B. stearothermophilus* and *L. lactis*; the major fluctuations concern regions connecting

Table 1. *Sequence of the Loop for different Fpgs:* Llactis *(Serre et al. 2002),* B. stearothermophilus *(Fromme and Verdine 2003),* T. thermophilus *(Sugahara et al. 2000), and* E. coli *(Gilboa et al. 2002)*

L. lactis	G	S_{217}	S	I	R			T	Y	S		A	L_{225}		G	S	T	G
B. stearothermophilus	G	S_{220}	T	V	R			T	Y	V		N	T_{228}	Q	G	E	A	G
T. thermophilus	G	S_{207}	T	L	S	D	Q	S	Y	R	Q	P	D_{218}		G	L	P	G
E. coli	G	T_{214}	T	L	K			D	F	L	Q	S	D_{223}		G	K	P	G

For each model, the corresponding X-ray numbering is used. Missing residues in X-ray models are underlined.

secondary structures. In bsoxo, the mean calculated B-factor for the Loop stays close to the average B-factor for this model (9 $Å^2$) and the same behavior is observed in *B. stearothermophilus* structure, where the Loop fluctuates like the rest of the backbone (average of 26 $Å^2$). In the *B. stearothermophilus* X-ray model, the major peaks correspond to residues 88–89 and 151–154, features also seen in bsoxo. Although the freeout and freein B-factors are similar, some differences can be observed: region 230–234, especially residue Asp 233, fluctuates above the average only in freein (twice the average for 230–232, 234; five times the average for 233). There is also a difference in the first three residues that are twice more flexible in freeout than in freein. In *L. lactis*, the available relative Loop B-factors are twice higher than the equivalent zone in the *B. stearothermophilus* X-ray structure. The region surrounding the missing residues 220–223 in *L. lactis* Fpg shows the highest peaks, up to twice the overall average, which might explain why it was not defined by crystallography. As in the *L. lactis* model, the Loop fluctuates twice as much as the average in the freeout model, whereas it fluctuates at about the average in the freein model.

To evaluate the stability of the models during the MD simulations, we also calculated the root mean square coordinate deviation of the protein and DNA backbones (P-C5′-C4′-C3′-O3′) from the initial structure, along the dynamics. In all three models, freein, freeout, and bsoxo, the rmsd increases in the first stage of the dynamics and stabilizes in the last nanosecond. The mean rmsds and associated standard deviation during the last nanosecond are equal to 1.35 ± 0.17 Å, 1.50 ± 0.10 Å, and 1.35 ± 0.13 Å for freein, freeout, and bsoxo, respectively.

For all three models, the end points of the DNA are very agitated, which is also the case in the X-ray structures. The rmsd is reasonable and the models remain stable despite the removal of half the base pairs for the freein and freeout models.

Dynamics within the damaged base cavity

In the absence of the base

The effect of the absence of the 8-oxoG moiety can be analyzed in the models freein and freeout. Water molecules are numerous in these two models as they invade the abasic site during the dynamics; as a consequence, few stabilizing hydrogen bonds involve the Loop atoms, which are maintained apart from the abasic site by water molecules. Only the Loop extremities are in contact with residues delimitating the cavity. In freeout, there are two hydrogen bonds between the nitrogen atoms of Ser 217 and Ser 218, and the carboxylate group of Glu 5. The Loop in freeout is also maintained by a hydrogen bond between N-Leu 225 and O-Tyr 79 that was present in the starting structure. In freein, three hydrogen bonds retain the Loop close to the active site. The interaction between Leu 225 and Tyr 79 and the one between N-Ser 217 and the carboxylate group of Glu 5 are present during the dynamics, whereas, as opposed to freeout, the one with Ser 218 does not occur. The O-Thr 221 and N_ζ-Lys 78 that were modeled close initially (2.15 Å) interact throughout the dynamics. This last interaction is not seen in freeout, where Thr 221 was initially built farther away from Lys 78 (~8 Å). The hydrogen bond present in the crystal structure between Glu 2 and Glu 5 is preserved during the simulations of freein and freeout. Besides, a hydrogen bond between O-Asp 233 and N-Lys 230 present in *L. lactis* occurs regularly during the dynamics of freeout, whereas it disappears after the first nanosecond in freein. This hydrogen bond loss in freein is correlated with the formation of a hydrogen bond between N_ζ-Lys 230 and O-Ser 218 of the Loop, not present in either the starting model of freeout or during its dynamics.

In the presence of the base

Figure 1, A–C, represents the hydrogen bond network between the 8-oxoG and the protein (water molecules not shown) for the oxosynin, the oxoantiin, and the bsoxo model, respectively, in their starting conformations and along the simulations. During the dynamics of the 8-oxoG-containing models of *L. lactis* Fpg, namely, the oxosynin, oxosynout, and oxoantiin models, there is no direct interaction between the Loop and the 8-oxoG, but water-mediated links are observed. In oxosynin, numerous water molecules form a hydrogen bond network that connect the Loop to the 8-oxoG, whereas in oxosynout only the extremities of the Loop are connected to the 8-oxoG via water molecules (data not shown). In oxosynin (see Fig. 1A), residues Glu 2 and Glu 5 interact with each other, the former interacting with the O_8 atom of the damaged base, and the latter being hydrogen bonded to N-Ser 217. Also, the Glu 76 entertains a strong hydrogen bond with the N_2 atom of the 8-oxoG while losing its starting interaction with Lys 78. Besides, the initial hydrogen bond between O_6 and $O_{\gamma 1}$ of Thr 221 is disrupted during the dynamics. In the oxoantiin model (Fig. 1B), the Loop remains close to the base and there are fewer water molecules than in the oxosynin model. Remarkably, a conserved water molecule ensures an interaction between the O_6 of the 8-oxoG and O-Ser 217, and one to two water molecules maintain the O_8 interacting with the carboxylate group of Glu 76. Besides, a hydrogen bond is formed during the dynamics between the carboxylate group of Glu 5 and the N_1 atom of the 8-oxoG. Thus, in oxoantiin the Loop is indirectly connected to the damaged base via Glu 5 that interacts with both the 8-oxoG and Ser 217. Also as in oxosynin, Glu 2 interacts both with Glu 5 and 8-oxoG (the N_2 atom in the *anti* conformation and the O_8 atom in the *syn* conformation). During the dynamics of oxoantiin, Glu 76

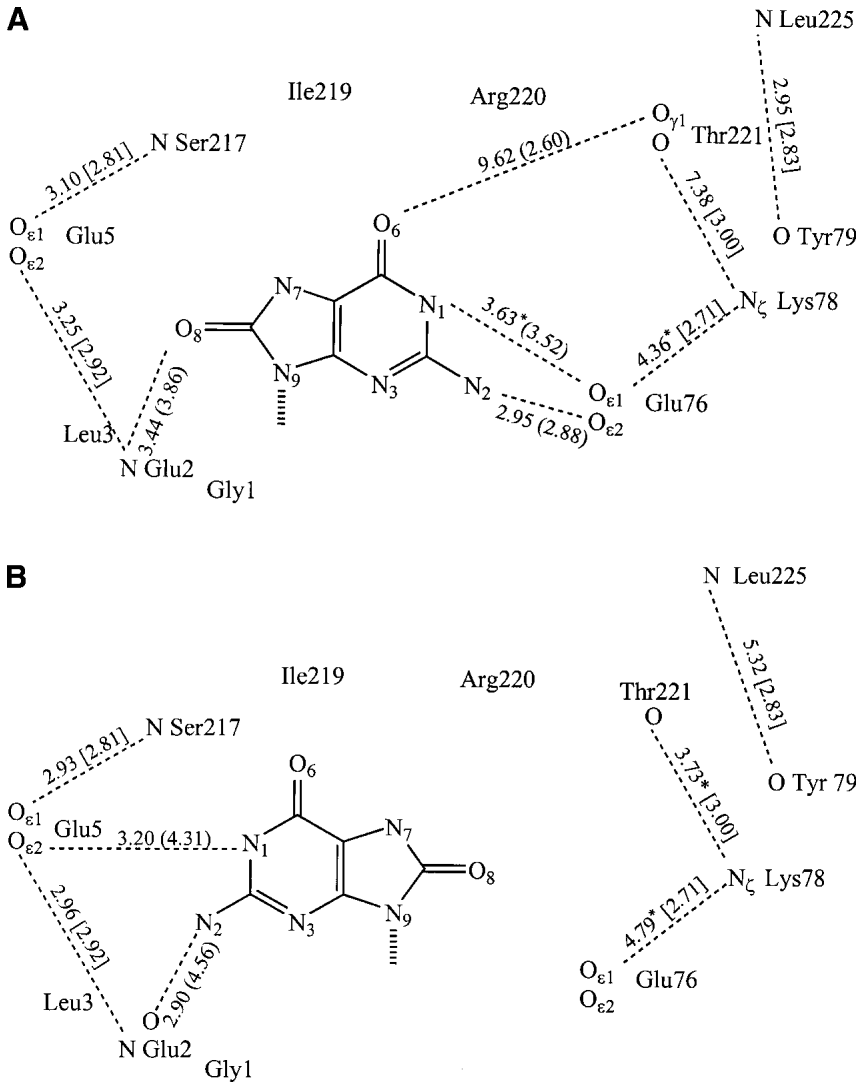

Figure 1. (Continued on next page)

loses its interaction with Lys 78 and is held close to the O_8 atom (mean distance is 3.44 Å), indicating a possible interaction if it was protonated. The hydrogen bond between Thr 221 and Lys 78, present in freein and oxoantiin, is absent in oxosynin. The interaction between Leu 225 and Tyr 79, seen in freein and oxosynin, is not observed in the oxoantiin model.

The active site in the *B. stearothermophilus* X-ray structure reveals numerous hydrogen bonds between the protein and the 8-oxoG and most of them are maintained during the dynamics of the bsoxo model, as seen in Figure 1C. All polar atoms of the 8-oxoG are involved in hydrogen bonds with surrounding protein residues. Water molecules are absent from the damaged base site crystal structure and do not play the role of hydrogen bond relays during dynamics as opposed to what is observed in oxosynin, oxosynout, and oxoantiin.

The 8-oxoG stays firmly positioned throughout the MD simulation; its N_7, O_6, and N_1 atoms are hydrogen bonded with Ser 220_{bs}, Arg 223_{bs}, and Thr 224_{bs} residues; its O_8 atom is hydrogen bonded to residues Glu 6_{bs} and Gln 3_{bs} (Glu 5 and Glu 2 in *L. lactis*); and its N_2 atom entertains stable hydrogen bonds with Glu 78_{bs} and Arg 223_{bs} (Glu 76 and Arg 220 in *L. lactis*). Among the three hydrogen bonds that were retaining the O_6 atom in the X-ray structure, one disappears along the dynamics (involving the main chain nitrogen of Val 222_{bs}), and the other two are weakened (involving the main chain nitrogens of Thr 224 and Tyr 225_{bs}). However, the Loop remains strongly stabilized along the MD, through hydrogen bonds with the 8-oxoG and with other protein residues, notably the one involving residues Thr 224_{bs} and Arg 80_{bs}. Besides, a strong hydrogen bond between residues Thr 224_{bs} and Glu 78_{bs}, present in the crystal structure, remains throughout the dynamics and

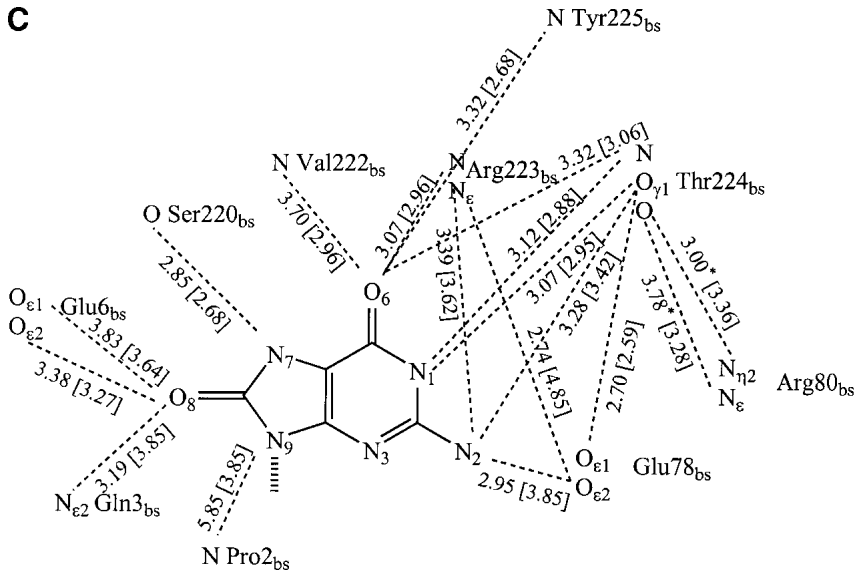

Figure 1. Hydrogen bond network between the protein residues and the 8-oxoG in (*A*) the oxosynin model, (*B*) the oxoantiin model, and (*C*) the bsoxo model. The mean distances over the last nanosecond dynamics are indicated, with an asterisk when the standard deviation is larger than 0.5 Å. Distances in square brackets refer to values in the corresponding crystal structures; distances in parentheses refer to the distances in the starting models. All distances are given in Angstroms.

is absent from the models derived from *L. lactis* (corresponding Thr 221 and Glu 76 residues). A stabilizing salt bridge for the Loop, involving residues Arg 223_{bs} and Glu 78_{bs}, appears during the dynamics and is also absent between the corresponding Arg 220 and Glu 76 in our models built from *L. lactis* Fpg.

In wild-type Fpgs, the nucleophile attack at the C_1' of the 8-oxoG by the N-terminal proline amino group is required to excise the damaged base. The corresponding glycosylase activity is, however, conserved for the P1G mutant from *L. lactis* (Serre et al. 2002) as opposed to the E3Q mutant from the *B. stearothermophilus* enzyme that is deficient in glycosylase activity. The evolution of the distance between the C_1' atom of the 8-oxoG and the amine nitrogen of the first residue along the dynamics is shown in Figure 2. In the bsoxo model, a major rearrangement is visible from this distance that goes from 3.46 Å in the *B. stearothermophilus* X-ray structure to a mean value equal to 5.35 ± 0.35 Å in the simulation. Moreover, it is always above 4.5 Å during the dynamics. In oxosynin, this distance fluctuates as well, around its mean value 4.63 Å, but, in contrast to bsoxo, it reaches 3.2 Å several times during the dynamics. This fluctuation also correlates well with the crystallographic model of *L. lactis* solved at 1.8 Å, which exhibits a double conformation for Gly 1, corresponding to a long and a short distance between C_1' and the nitrogen atom of Gly 1 (4.11 and 2.60 Å). A similar pattern of fluctuations for this crucial distance is observed for the oxosynout model, except that it attains short values of 3.5 Å less frequently. In the oxoantiin model, as in the bsoxo model, this distance remains long with a mean value of 5.95 ± 0.33 Å much longer than in the oxosynin and oxosynout models.

Dynamic behavior of the Loop

The rmsd (from the starting structure) of the protein and DNA backbones for all models increases during the first

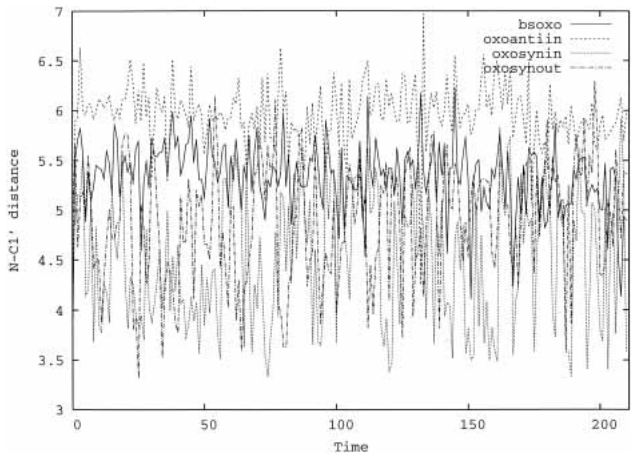

Figure 2. Distance between the nitrogen atom of Pro 2_{bs} and the C_1' atom of the 8-oxoG in bsoxo and the corresponding distance between the nitrogen atom of Gly 1 and the C_1' atom of the 8-oxoG in oxosynin, oxosynout, and oxoantiin during the last nanosecond dynamics. The distance and the time are given in Angstroms and in nanoseconds, respectively.

500 psec and then stabilizes to values between 1.3 and 1.5 Å for freein, freeout, and bsoxo, as stated previously. For the oxosynin, oxosynout, and oxoantiin models, the rmsd increases gradually up to 1.6 Å.

To examine the relative role of the Loop flexibility in these overall rmsd, the rmsd of the Loop heavy atoms were calculated along the dynamics, as illustrated in Figure 3. The largest and most unstable deviation of the Loop occurs in the oxosynin model; initially ~2.5 Å, it jumps up to 3.25 Å at ~1.1 nsec, so the MD simulation for this model was continued up to 3 nsec. After 2.7 nsec, the rmsd of the Loop decreases to ~3.5 Å, where no clear stabilization is observed, indicating that the Loop in the starting model was quite far from a stable conformation—if there is any for this model—compared with all other models. For the last nanosecond of this 3-nsec run, the mean rmsd of the Loop is equal to 4.04 ± 0.34 Å. The rmsd of the Loop in the oxoantiin model is ~2.5 Å for the first 1.5 nsec; then, as opposed to oxosynin, there is no real jump and the mean deviation for the last nanosecond is 2.77 ± 0.23 Å. The Loop shows the least flexibility in the bsoxo model, with a mean rmsd at 0.89 ± 0.16 Å for the last nanosecond. Besides that, it contributes very little to the overall rmsd. In the freein and freeout models, the Loop attains a stable rmsd after the first 500 psec with a mean deviation of 2.00 ± 0.17 Å and 2.54 ± 0.33 Å, respectively. The rmsd of the Loop in oxosynout increases at the beginning of the dynamics and stabilizes around the mean value of 1.76 ± 0.21 Å.

The differences in the dynamic behavior of the Loop can also be examined through the atomic fluctuations relative to the average fluctuations of the entire protein backbone, given in Table 2. The stabilization of the Loop residues

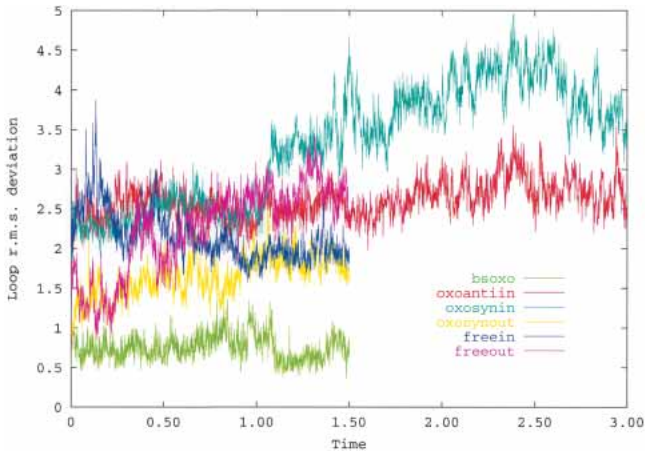

Figure 3. Rmsd of the backbone atoms within the Loop for all models, calculated along the whole trajectory with respect to the starting X-ray model structure for *L. lactis*-derived models (oxosynin in cyan, oxosynout in yellow, oxoantiin in red, freein in purple, and freeout in magenta) and bsoxo (in green). The rmsd and the time are given in Angstroms and in nanoseconds, respectively.

220_{bs}-228_{bs} in *B. stearothermophilus* is clearly seen from their mean atomic fluctuations, lying between 0.6 and 1.24 relative to the average fluctuation of the whole enzyme heavy atoms. These fluctuations are comparable to those in bsoxo, in both cases around the average value (the same as in the *B. stearothermophilus* model). The fluctuations of the Loop residues are somewhat lower in the MD simulation of bsoxo than in its crystal counterpart. In the models built from *L. lactis* Fpg, the Loop is much more agitated. In oxosynout and freeout, the fluctuations are above the average, especially in the region not seen by crystallography (220–223). The Loop of the freein model fluctuates to a lesser extent, and in the oxosynin model, its fluctuations decrease from 1.5 nsec to 3.0 nsec but are still large compared with the average. This last observation might indicate that this model is not stabilized yet or cannot be stabilized. In the oxoantiin model, as opposed to the oxosynin case, the Loop fluctuations are low, around the average (between 0.5 and 1.3), as in the bsoxo model.

Correlated motions along the dynamics

For the six Fpg models, we analyzed the correlated motions during the last nanosecond of the dynamics simulation. Covariance plots of the C_α atomic fluctuations are shown in Figure 4.

The covariance plot of the bsoxo model shows that the enzyme is dynamically divided into two domains according to the correlated C_α atomic displacements. The first one contains residues 2_{bs}-130_{bs}, the second one contains the two subdomains, residues 135_{bs}-218_{bs} and residues 235_{bs}-274_{bs}. Both subdomains of the C-terminal domain exhibit anticorrelated motion with the first domain and the Loop. In oxosynout, similar patterns are observed with the corresponding domains of *L. lactis* Fpg. This domain pattern is also present to a lesser extent in freeout, oxosynin, and oxoantiin plots, as shown in Figure 4. A common feature observed in bsoxo and oxosynout only is the strong anticorrelated motion of the N-terminal domain and of the zinc subdomain. On the contrary, in the covariance plots of oxosynin, oxoantiin, and freeout, practically no anticorrelated motions of the two C-terminal subdomains with the first domain are observed. Globally, the covariance plot of oxoantiin is very similar to the one of oxosynin. In freeout, and to a lesser extent in oxosynin and oxoantiin, there is a positive correlation, absent in bsoxo and oxosynout, between most of the C-terminal domain and regions of residues 50–60 and 70–80. The covariance plot of freein is very different from all others. There are few significant anticorrelated motions. The domains are not clearly delineated and several zones alternate strong correlation (turns at the domain interface) or no correlation. The C-terminal subdomains exhibit dynamic behavior as a whole compared with the other models.

Table 2. *Mean atomic fluctuations of the Loop residues (backbone atoms only) relative to the average fluctuations of the protein backbone given for all our models during the last nanosecond dynamics compared with both X-ray model values*

B. stearothermophilus	219_{bs}G	220_{bs}S	221_{bs}T	222_{bs}V	223_{bs}R	224_{bs}T	225_{bs}Y	226_{bs}V	227_{bs}N	228_{bs}T
B. stearothermophilus	0.86	0.83	0.93	1.04	1.21	1.06	0.92	0.89	1.03	1.17
Bsoxo	0.68	0.59	0.74	0.87	0.93	0.85	0.94	1.06	0.97	1.24
L. lactis	216G	217S	218T	219I	220R	221T	222Y	223S	224A	225L
L. lactis	1.15	1.45	1.89	N/A	N/A	N/A	N/A	2.17	1.75	1.79
Freein	1.01	0.86	1.77	2.12	2.51	1.39	1.06	1.22	1.34	1.01
Freeout	0.91	1.11	1.62	1.82	2.49	3.26	2.79	2.46	1.90	1.76
Oxosynin (1)	0.70	0.78	1.26	1.84	4.06	5.18	3.06	2.46	0.97	0.74
Oxosynin (2)	0.87	1.06	1.38	2.01	2.71	3.07	1.84	1.52	0.88	0.78
Oxoantiin	0.52	0.52	0.64	0.73	1.08	1.25	0.78	0.74	0.59	0.57
Oxosynout	0.58	0.60	0.80	1.26	2.61	3.95	7.71	2.94	1.36	1.08

For the oxosynin model, two sets are given corresponding to different periods of the dynamics (1) from 1.5 to 2.5 nsec and (2) from 2.0 to 3.0 nsec.

The Loop 220_{bs}-228_{bs} in bsoxo shows a correlated motion with the first domain and an anticorrelated motion with the two C-terminal subdomains, as seen in oxosynout. This echoes the crystal structure, where this Loop is included in a large nonregular segment, part of it covering some residues of the N-terminal domain. In freeout, oxosynin, and oxoantiin, the Loop shows some correlated motion with the first domain but no correlation with the two C-terminal subdomains. The Loop covariance plot in freein is different from all other models, as it shows a correlation with most of the protein. In the oxoantiin model, there are more correlated motions between the region around the Loop and the first domain than in the oxosynin model.

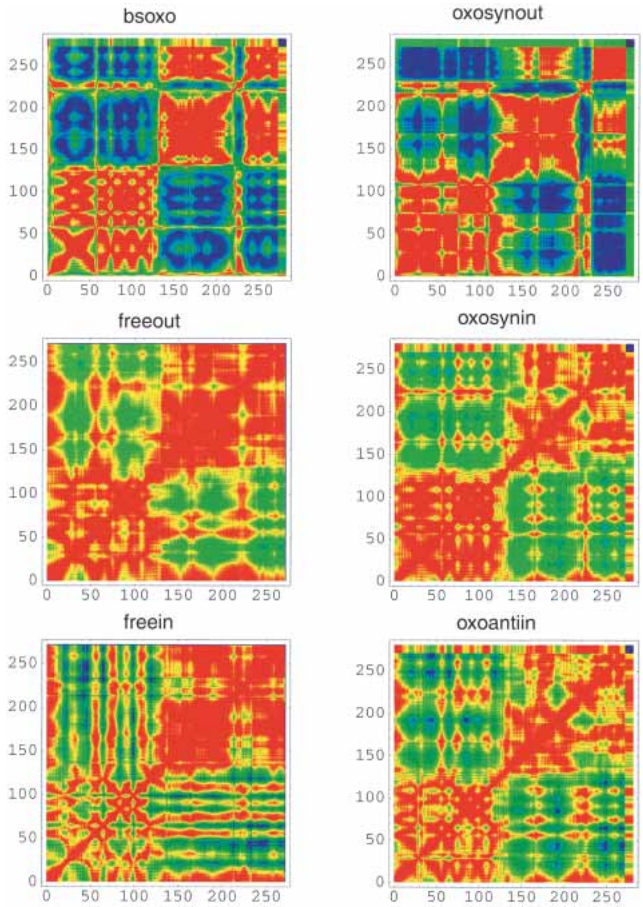

Figure 4. Covariance matrices for the fluctuations of the C_α atoms in the models bsoxo, oxosynout, freeout, oxosynin, freein, and oxoantiin. For clarity, the oxo-correlated values with the rest of the protein are amplified and shown in region 273–283 for bsoxo and 271–281 for oxosynout, oxosynin, and oxoantiin. The correlation goes from −1 to 1 from blue to red.

The presence of the 8-oxoG, independently of the Loop conformation, induces a clear scheme of correlated motion of the two domains (see Fig. 4) for bsoxo, oxosynout, and to a lesser extent for oxosynin and oxoantiin. The Loop has a positive correlated motion with the N-terminal domain when the 8-oxoG is bound into the protein. The correlation fluctuations of the 8-oxoG with the protein residue are depicted in Figure 5. Among the four models containing the damaged nucleotide, the 8-oxoG ligand exhibits strong positive correlations in oxoantiin (from 0.6 to 1) and oxosynin (from 0.1 to 1). In bsoxo, it explores a larger range of covariance values (from −0.4 to 0.8) and therefore more diverse motions relative to the protein. In contrast, the damaged base motions in oxosynout are not correlated with the motions of the enzyme. If we consider bsoxo, oxosynin, and oxoantiin, that is, the models with the Loop located toward the protein interior, the damaged base displacements are positively correlated with the displacements of (1) the first N-terminal residues, (2) the regions surrounding the three intercalated residues (Met 75, Arg 109, Phe 111 in *L. lactis*), (3) the regions involved in the recognition of the phosphate backbone on the lesion containing DNA strand (around 57–60, 170–175, 250–260), and (4) the first N-terminal residues of the Loop. Bsoxo exhibits anticorrelated motion between the 8-oxoG and some residues of the enzyme: weak negative covariances are observed with the C-terminal part of helix A and regions that are in close contact at the surface of the N-terminal domain, far from the DNA binding site.

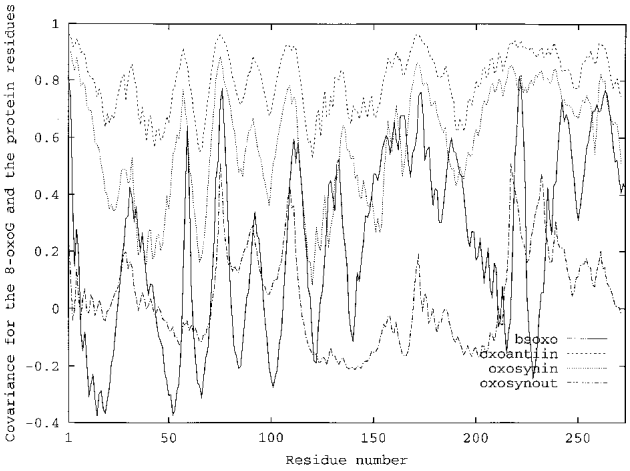

Figure 5. Covariance for the 8-oxoG with the protein residues for models bsoxo, oxosynout, and oxoantiin.

When the Loop points toward the base (oxosynin, oxoantiin, or bsoxo) or toward the solvent (oxosynout), a clearly distinct pattern is observed for residues ranging from 150 to 190, that is, for the H2TH motif. The damaged base is strongly correlated to this motif when the Loop points toward the base, and in oxosynout there is practically no correlation.

Average structures of the Loop

A view of the averaged Loop structures (over the last nanosecond dynamics) for bsoxo, oxoantiin, oxosynin, and oxosynout is shown in Figure 6. The superposition represented corresponds to the best fit calculated on 230 C_α pairs with the O program and the LSQ option (Jones et al. 1991). The Loop in bsoxo and oxoantiin is close to the 8-oxoG, even though in this latter case only, there is no direct interaction between both parts. In these two models, the Loop adopts a conformation similar to that found in the DNA free model of *T. thermophilus* X-ray structure. As opposed to the Loop in oxoantiin, the Loop in oxosynin, initially docked in the vicinity of the 8-oxoG, has moved away from the damaged base site to the location of the Loop in the oxosynout model, even though their global average fold is different. In the last nanosecond, the Loop in oxosynin and oxosynout has evolved toward a position similar to freeout, whereas the Loop in bsoxo and oxoantiin remains in a position close to the one observed in freein (data not shown). The only difference in the freein and freeout average structures lies in region 220–224, which points toward the cavity in freein and toward the protein surface in freeout, similar to what was modeled initially. Of these two models, the freein average structure resembles most the *T. thermophilus* Fpg where the Loop occupies partially the location of the 8-oxoG. The fold of the Loop in *T. thermophilus* Fpg shows the greatest similarity with the one of bsoxo and to a lesser extent with the oxoantiin, as opposed to the equivalent region in oxosynin and oxosynout.

Discussion

Numerous X-ray structures of bacterial Fpg provide snapshots of the catalytic cycle performed by this DNA repair enzyme even though no active enzyme bound to a true substrate, that is, an 8-oxoG containing DNA, is known. Indeed, X-ray models are available either in the native or mutant form, free or bound to damaged DNA with lesions like 8-oxoG or with abasic sites. Among these snapshots, an intriguing feature is the conformation adopted by the short polypeptide (10 to 12 residues) connecting together the H2TH and the zinc finger subdomains. This region, called the Loop in this study, is well defined in the free enzyme structure from *T. thermophilus* (Sugahara et al. 2000) and in the complex formed by the 8-oxoG containing DNA and a glycosylase-deficient mutant Fpg from *B. stearothermophilus* (Fromme and Verdine 2003). However, it is partially disordered in all of the crystal structures of Fpg complexed with abasic site containing oligomers, independently of the source of the enzyme (Fromme and Verdine 2002; Gilboa et al. 2002; Serre et al. 2002). This disorder is also observed in the *E. coli* EndoVIII covalently bound to an abasic site containing DNA (Zharkov et al. 2002), and thus could be a hallmark of the structural family defined by Fpg. Whether the disorder of the Loop might be related to a catalytic event during the overall repair pathway has been examined in this study by MD simulations conducted on six models. Five models derived from the AP lyase-deficient mutant *L. lactis* enzymes were built, either bound to an 8-oxoG nucleotide in *syn* and in *anti* conformation or to an abasic site, as well as a model of the glycosylase-deficient mutant Fpg from *B. stearothermophilus.* The 8-oxoG-bound models and the abasic site models could mimic the step just preceding the glycosylase reaction and the product of this reaction, respectively. We analyzed the dynamics of these models in relation to the presence or absence of the damaged nucleotide.

Dynamical behavior of the Loop

In the crystal structure of *B. stearothermophilus* Fpg, the fluctuations within the Loop are similar to the average fluctuations of the rest of the protein, which is easily explained by the numerous hydrogen bonds capping the 8-oxoG. In contrast, in the *L. lactis* model, part of the Loop is missing and the defined residues fluctuate up to twice the average value. This phenomenon is observed for the *L. lactis*-derived models oxosynin, oxosynout, and freeout and to a lesser extent in freein, whereas the Loop is stabilized in the oxoantiin model. The freeout model appears to be more

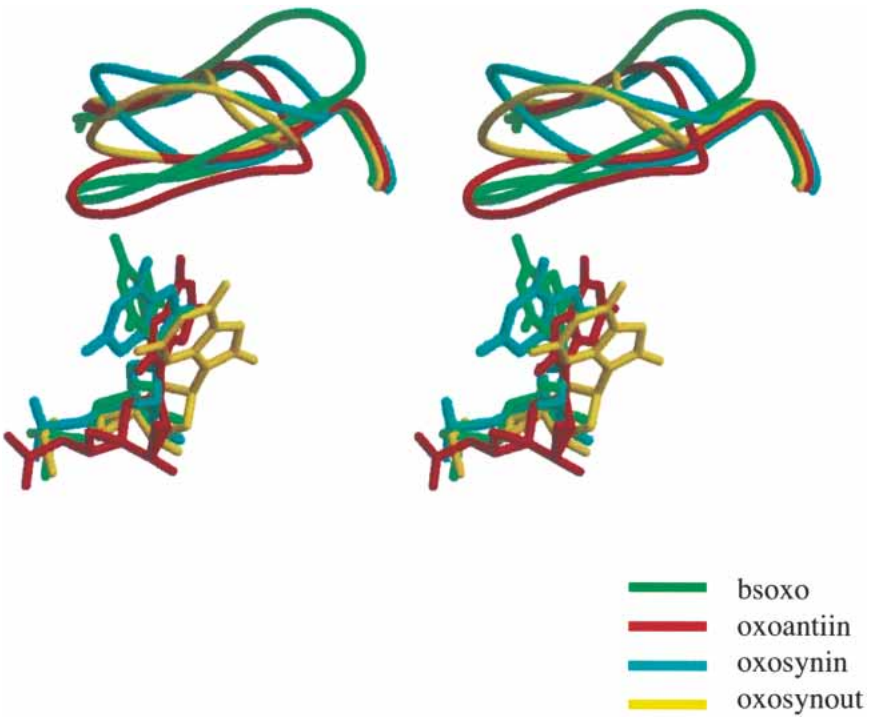

Figure 6. Superposition of the averaged structures over the last nanosecond dynamics for bsoxo (in green), oxoantiin (in red), oxosynin (in cyan), and oxosynout (in yellow).

representative of the *L. lactis* crystal structure than the freein model according to the strong fluctuations of residues 218–228 of the Loop in the freeout model that might explain why this region did not correspond to a well-defined electron density in the crystallographic model. In the oxosynout model which has the same starting model for the Loop as freeout, residues ranging from 220 to 223, and particularly Tyr 222, are agitated. Thus, when the Loop is "out", the presence of the 8-oxoG is not sufficient to stabilize the structure of peptide 220–223. When the conformation of the Loop is "in" as in the oxosynin model, the results are less clear because the Loop fluctuations remain high even after 3.0 nsec, and the Loop does not keep its initial position either. The behavior of the Loop in oxosynin is therefore very different than in bsoxo; in both cases, it is initially located close to the 8-oxoG but in the former, it never gets bound to it in the dynamics simulation time. On the contrary, the Loop motions in oxoantiin are reduced as the Loop is held close to the 8-oxoG either by water-mediated hydrogen bonds or by an indirect interaction via Glu 5. In *L. lactis* models, with the exception of the oxoantiin model, the Loop region fluctuates much more than in bsoxo. Comparing the average structures (Fig. 6) reveals that, during dynamics, the Loop in oxosynin adopts the location of the one in oxosynout, similar to the Loop average structure of freeout. Consequently, if the 8-oxoG is present in the binding pocket under the *syn* conformation, the Loop seems to stabilize in the position it occupies in the freeout model, toward a complex between Fpg and an abasic site containing DNA. This could result from the state of the whole starting structure (after base excision) that does not allow the association of a *syn* 8-oxoG and the "in" Loop conformation.

The domain delineation related to the presence of the 8-oxoG

The correlated motions of the protein analyzed for the four models containing the 8-oxoG indicate that the presence of the 8-oxoG is crucial in the definition of the different domains and subdomains (Fig. 4). Thus, the presence of the damaged base leads to opposite motions of the N- and C-terminal domains. The binding of the 8-oxoG is also related to the positive correlated motions between the Loop residues and the N-terminal domain. Indeed, when the enzyme is bound to an abasic site as in the *L. lactis* X-ray structure whose dynamic behavior is best modeled by freeout, the correlations are attenuated. This difference could be correlated to the reactivity of the enzyme: when the 8-oxoG is bound, concerted motions of the two domains and of the Loop may be required either to confirm the recognition of the damaged base or to allow the excision and expulsion of the 8-oxoG. However, to process an AP site, these concerted movements would not be necessary. Interestingly, when Fpg binds to an AP site, the Loop loses the original con-

formation adopted in the free enzyme (as in the *T. thermophilus* structure). Therefore, one may wonder whether the ligand stabilizes the Loop or the Loop stabilizes the ligand.

In freein, the conjugation of the Loop insertion and the absence of the 8-oxoG has a strong impact on the N-terminal domain that does not exhibit a dynamic behavior as a whole. This could indicate that freein does not correspond to any snapshot of the overall catalysis.

On the relative motions of the Loop and the 8-oxoG

The correlated motions of the 8-oxoG and the protein residues are strong for the models with the Loop inside the protein and quasi null when the Loop is outside, indicating that the position of the Loop has a significant effect on the motions of the 8-oxoG.

The X-ray model of bsoxo reveals an important hydrogen bond network between the Loop and the 8-oxoG, in favor of the hypothesis in which the Loop and the ligand motions would be intimately related. During the dynamics, most of this network is maintained, which, combined with our results on the oxosynin, oxosynout, and the oxoantiin models, strongly suggests that the Loop plays a major role in the dynamic behavior in the vicinity of the 8-oxoG. In the oxosynin, oxoantiin, and bsoxo models, the damaged base motions are correlated with the residues involved in the catalysis, in the DNA intercalation, in the recognition of the opposite cytosine, and with Loop residues. In bsoxo, the Loop is clearly bound to the 8-oxoG and as a consequence was proposed to recognize the damaged base specifically. The same correlations for the 8-oxoG are observed in the oxosynin and oxoantiin models, but the specific recognition role is less clear because the Loop and the 8-oxoG-specific atoms (H_7 and O_8) interact only via ordered water molecules for both models; the only connection via Glu 5 and Glu 2 for the oxoantiin model involves the N_1 and N_2 atoms that are not specific of the oxidized base. This discrepancy between our *L. lactis* models and the bsoxo model could arise from the use of a glycosylase-deficient mutant in bsoxo. The inactive enzyme model shows a somewhat rigid behavior at the damaged site with a strong dynamic delineation of the protein domains, whereas the glycosylase active models are more flexible. The tight binding between the Loop and the 8-oxoG in bsoxo would correspond to a cul-de-sac, the Loop being locked against the damaged base as if something would prevent the base excision. This situation resembles, interestingly, the oxoantiin case where the Loop is retained in the initial conformation, close to the damaged base. Therefore, modeling an 8-oxoG in the *anti* conformation in *L. lactis* Fpg would be similar to a complex with an inactive enzyme. It would not lead to the base excision coupled to the Loop mobility on a glycosylase functional enzyme.

Different behavior of bsoxo and oxosynin

The *B. stearothermophilus* 3D structure is highly homologous to the *L. lactis*. Despite this homology, the oxosynin and the bsoxo dynamics show distinct interactions at the active site. Different explanations here might be invoked for these differences. First, the dynamics simulation might not have been long enough for our model to reach a conformation in which the backbone atoms of the Loop residues would be involved in the 8-oxoG stabilization. This would imply that the abasic X-ray model we started from is globally quite far from the bsoxo model and that more rearrangements would be necessary to recover a bsoxo-like structure.

Another alternative would be that, during the dynamics, the system has reached a stable conformation, which implies that the Loop farther away from the 8-oxoG after 1 nsec (in the location of the Loop in oxosynout) will not get back close enough to the 8-oxoG for a binding similar to what is seen in bsoxo. This would suggest that the X-ray structure of the abasic site might be an irreversible conformation which cannot come back to an 8-oxoG-containing structure (bsoxo-like) by simply docking the missing Loop and the oxoguanine at the abasic site. In favor of this last hypothesis, it was proposed that the DNA glycosylase and AP lyase activities of bifunctional DNA glycosylases such as Fpg and its human functional homolog, hOgg1, are actually decoupled and require structural rearrangements between the two catalytic processes (Vidal et al. 2001). After the excision of the oxidized base (i.e., DNA glycosylase activity), hOgg1 would, in most cases, dissociate from the resulting AP site without engaging in the AP lyase process and the cleaved oxidized base would be expulsed from the extrahelical base binding pocket. Then, hOgg1 would be able to rebind to the AP site and cleave the DNA. Despite the displacement of the Loop away from the 8-oxoG in oxosynin, water-mediated interactions with the 8-oxoG (O_6, O_8, N_7) somewhat hold them together. This "soft" binding mode might be the favored conformation for the Loop before the 8-oxoG is excised. Indeed, tight interactions with the damaged nucleotide can hinder an efficient catalytic process, strongly decreasing the enzyme turnover.

This difference between *L. lactis* and bsoxo models could also translate a substrate recognition that would be species dependent. Indeed, the difference between the strong binding of the 8-oxoG in bsoxo as opposed to what is observed in all *L. lactis*-derived 8-oxoG models could come from the added residues in the sequence of the Loop in bsoxo. In addition, the thermophile character of *B. stearothermophilus* Fpg, which is active at 323K, would be responsible for a higher Loop rigidity at 300K, the temperature used for the dynamics simulation.

Finally, from the differences between *L. lactis*-derived models and bsoxo, could also arise the questionable rel-

evance of modeling an 8-oxoG in an abasic site X-ray structure. Besides, we have studied models from, on one hand, an inactive enzyme (bsoxo), and on the other hand, an active enzyme (*L. lactis* models), regarding the glycosylase activity.

Dynamic behavior of Fpg models related to catalysis

Our results can be related to catalysis, bearing in mind that (1) the *B. stearothermophilus*-derived model is a glycosylase-deficient mutant, (2) the *L. lactis*-derived models are deprived of a damaged base, and (3) Glu 2, involved in the catalysis, is deprotonated in our models. We found that the binding of the Loop with the damaged base in the *syn* conformation is stable during the 1.5-nsec dynamics, and our study supports a specific recognition of the *syn* 8-oxoG by *B. stearothermophilus* Fpg. Interestingly, in the bsoxo dynamics, the distance between the amine nitrogen of Pro 2_{bs} and C_1' of the damaged base is always above 4.5 Å (Fig. 2), too long for a favorable nucleophilic attack, a result that can be correlated with the glycosylase deficiency of this mutant. Thus, something in the surrounding of the 8-oxoG prevents the catalytic Pro 2 and the C_1' of the 8-oxoG from being brought together in the mutant of the *B. stearothermophilus* enzyme. The crystal structures of the trapped complex Endo VIII (Zharkov et al. 2002) or *E. coli* Fpg (Gilboa et al. 2002) have shown the importance of Glu 3 (Glu 2 in *L. lactis*) in the stabilization of the reduced sugar in C4′-OH, an event supposed to occur before the base excision (Castaing et al. 1999). This would not be possible with the E3Q mutation, and the nonexcision of the base is certainly due to the mutation (Lavrukhin and Lloyd 2000). In this mutant, if the 8-oxoG cannot be excised, the Loop remains tightly bound to the damaged base. The dynamics of the oxosynin model shows that the distance between the Gly 1 amino group (corresponding to Pro 2_{bs} in *B. stearothermophilus*) and C_1' ranges from 3.2 to 5.5 Å, which correlates well with the biology (the mutant P1G is still glycosylase active) and with the double conformation of Gly 1 modeled in the crystal structure. The fact that the nucleophilic attack is possible, together with the fact that the Loop is softly bound to the 8-oxoG via water-mediated hydrogen bonds, allowing the base extrusion in a following step, is in favor of a *syn* binding mode for the *L. lactis* Fpg. On the contrary, when the 8-oxoG model is bound in the *anti* conformation, this distance is always ~6 Å, far from a possible interaction. The tighter binding of the Loop to the 8-oxoG and the long distance between the Gly 1 amino group and the C_1' observed in the *anti* simulation versus the *syn* converge to the same conclusion, that is, that the *anti* conformation might not be functional if the Loop flexibility is relevant for the glycosylase activity. Surprisingly, the oxoantiin model is closer to the bsoxo model than the oxosynin model, even though in the *B. stearothermophilus* enzyme the 8-oxoG is bound in *syn* conformation. Zaika et al. (2003) suggested that the *syn* binding could be an artefact and that from their dynamics simulation of *E. coli* Fpg the *anti* binding mode was favored, although in their paper no explicit dynamic behavior of the Loop with respect to the 8-oxoG *syn* or *anti* is described, which prevents a systematic comparison with our findings for *L. lactis*.

The authors favor the *anti* conformation by similarity with hOgg1 (Bruner et al. 2000) and because mutation of Lys 217_{ec} residue present in the Loop reduces the 8-oxoG excision ability of Fpg; the important role of this residue was suggested by their simulation model in which Lys 217_{ec} interacts with the O_8 of the damaged base. However, the effect of this mutation is not significant enough (5-fold decrease compared with a 500-fold decrease in E3Q mutant; Lavrukhin and Lloyd 2000) to conclude that Lys 217 is critical for the base recognition. In addition, the authors mention that the side chain of Arg 223_{bs}, the equivalent residue in the X-ray model of *B. stearothermophilus* Fpg, is not close to the damaged base in *syn* conformation, which is surprising as the N_ε is initially at 3.62 Å of N_2 and at 4.85 Å of the carboxylate group of Glu 78_{bs}, which is itself hydrogen bonded to N_2. Besides, during the dynamics, Arg 223_{bs} remains in the vicinity of the damaged base (Fig. 1C). In oxosynin and oxoantiin, the corresponding Arg 220 is ~6 Å from the 8-oxoG with no direct interaction observed during dynamics.

Even though the simulation times in the present study are on the order of the nanosecond and thus might not grasp all the significant dynamical features of the different models, we found that these simulations imply that the *syn* conformation of the 8-oxoG is favored over the *anti*, in agreement with the X-ray structure of *B. stearothermophilus* and with a catalytic role for the flexibility of the Loop region. The variation of flexibility observed between *L. lactis* and *B. stearothermophilus* models could also reflect species-dependent differences (thermo-sensibility, inactive mutant).

Materials and methods

Structural models

The crystal structure of the *L. lactis* formamidopyrimidine-DNA glycosylase bound to an abasic site analog-containing DNA refined at 1.8 Å (B. Castaing and L. Serre, pers. comm.) was used as our starting model for all of the Fpg–DNA complexes. We will refer to this structure as *L. lactis* Fpg. Missing residues (220–223) of the disordered Loop in *L. lactis* Fpg were constructed with the program Insight II (Accelrys, Inc.). Two possible conformations of the Loop were modeled, taking into account that the Tyr 222 side chain could either point toward the active site (according to what is seen in *T. Thermophilus* and *B. stearothermophilus* Fpg structures) or not. This latter orientation, drastically different from the former, was constructed ab initio so as to mimic an alternate, solvent-exposed conformation. Each of these conformations was included in a model named "in" and "out", respectively (for the

Tyr 222 pointing inside the protein or toward the protein surface). Both models were simulated for the abasic (free) and the 8-oxoG-containing DNA (oxo), so that four systems were built, namely, freein, freeout, oxosynin, and oxosynout. We should mention at this point that when we started this study, no structural evidence had precluded either rotamers of the 8-oxoG, as no X-ray data were available at that time, and both conformations were possible (Serre et al. 2002). Thus, we investigated both the *anti* and the *syn* conformations of the 8-oxoG by setting the dihedral O_4'-C_1'-N_9-C_8 to 88 and −90°, respectively, without altering the rest of the system. The central nine bp of the crystal DNA double strand were included in our simulations. In light of the recently reported X-ray structure of *B. stearothermophilus* Fpg complexed to an 8-oxoG-containing DNA where the 8-oxoG is in *syn* conformation (Fromme and Verdine 2003), we performed the simulations with the base in this conformation (oxosynin and oxosynout). However, the recent publication on *E. coli* Fpg (Zaika et al. 2003) suggests that the binding of the 8-oxoG is more favorable in the *anti* conformation, so we performed a simulation with the base in this conformation, while the Loop is "in" (the oxoantiin model). Structural water molecules were included.

The molecular mechanics program CHARMM version 27 (Brooks et al. 1983; Mackerell et al. 1998) was used for all simulations. The parameters for the abasic site were assigned from standard parameters for methylene groups. Atomic charges for the 8-oxoG were fitted from electrostatic potential using the program Jaguar (Jaguar 4.2, Schrödinger, Inc)—the standard Hartree-Fock method with a 6–31G* basis set was used for this calculation. Hydrogens were added to the model using the HBUILD program (Brünger and Karplus 1988) implemented in CHARMM. The four cysteines, Cys 245, Cys 248, Cys 265, and Cys 268, were deprotonated to account for their interaction with the Zn^{2+} ion of the zinc finger domain.

The crystal structure of the 8-oxoG-containing DNA complex with *B. stearothermophilus* Fpg became available during this study (Fromme and Verdine 2003). A model was derived from this structure using the same procedure to build hydrogens and to solvate the enzyme. All 12 bp of the X-ray structure were taken into account. The model resulting from this modeling phase is called bsoxo.

Simulation protocol

The six resulting systems were placed in a box of water molecules of 80 $Å^3$. All water molecules (crystallographic or from the water box) within 2.8 Å of the DNA and the protein atoms were removed. Periodic boundary conditions were used to model the solvent. Sodium ions were automatically added to neutralize the DNA–protein complexes (Balaeff 2000). The six systems that consisted of ~32,000 atoms were then minimized to remove local steric hindrances. Initially, all atoms were held by harmonic constraints with force constants decreasing gradually to zero. The dynamic simulations were performed at constant pressure and temperature (1 atm and 300K). A time step of 1 fsec and the Leap Verlet algorithm was used to integrate the equations of motion. All atoms were allowed to move during the MD simulations except for the water molecule geometry that was kept fixed using SHAKE in CHARMM. A cutoff of 14 Å was used to compute nonbonded interactions. This value, larger than the standard cutoff of 12 Å, was chosen so that interactions between all atoms of the Loop and the 8-oxoG were included during the dynamics. The particle mesh Ewald algorithm (Essmann et al. 1995) was used to efficiently compute the electrostatic interactions. For each model, a 1.5-nsec dynamics was performed, but the trajectory was continued up to 3.0 nsec for the oxosynin and the oxoantiin models. In all trajectories, the last nanosecond was used for the analysis. All calculations were performed on 16 processors of HP SC45 (800 processors Alpha 1.25 GHz, quadrics network).

For clarity throughout the paper, the residue numbering corresponds to the X-ray structure from *L. lactis* enzyme except when the subscript bs is specified, referring to the X-ray structure of *B. stearothermophilus* enzyme or the subscript $_{ec}$ for the X-ray structure of *E. coli* enzyme.

Acknowledgments

We thank the Commissariat à l'Energie Atomique, the Centre de Calcul Recherche et Technologie (CEA, Bruyères-le-Châtel), and the Centre National de la Recherche Scientifique for support. B.C. thanks the Electricité de France (EDF) for support.

The publication costs of this article were defrayed in part by payment of page charges. This article must therefore be hereby marked "advertisement" in accordance with 18 USC section 1734 solely to indicate this fact.

References

Balaeff, A. 2000. SODIUM: A program for arranging ions around biological macromolecules. VERSION: 1.5.1, The Theoretical Biophysics Group, Beckman Institute, and The Board of Trustees of the University of Illinois.

Brooks, B.R., Bruccoleri, R.E., Olafson, B.D., States, D.J., Swaminanathan, S., and Karplus, M. 1983. CHARMM: A program for macromolecular energy, minimization, and dynamics calculations *J. Comput. Chem.* **4:** 187–217.

Bruner, S.D., Norman, D.P.G., and Verdine, G.L. 2000. Structural basis for recognition and repair of the endogenous mutagen 8-oxoguanine in DNA. *Nature* **403:** 859–866.

Brünger, A.T. and Karplus, M. 1988. Polar hydrogen positions in proteins: Empirical energy placement and neutron diffraction comparison. *Proteins* **4:** 148–156.

Castaing, B., Fourrey, J.L., Hervouet, N., Thomas, M., Boiteux, S., and Zelwer, C. 1999. AP site structural determinants for Fpg specific recognition. *Nucleic Acids Res.* **27:** 608–615.

Chetsanga, C.J. and Lindahl, T. 1979. Release of 7-methylguanine residues whose imidazole rings have been opened from damaged DNA by a DNA glycosylase from *Escherichia coli*. *Nucleic Acids Res.* **21:** 2899–2905.

Duarte, V., Gasparutto, D., Jaquinod, M., and Cadet, J. 2000. *In vitro* DNA synthesis opposite oxazolone and repair of this DNA damage using modified oligonucleotides. *Nucleic Acids Res.* **28:** 1555–1563.

Essmann, U., Perera, L., Berkowitz, M.L., Darden, T., Lee, H., and Pedersen, L.G. 1995. A smooth particle mesh Ewald method. *J. Chem. Phys.* **103:** 8577–8593.

Fromme, J.C. and Verdine, G.L. 2002. Structural insights into lesion recognition and repair by the bacterial 8-oxoguanine DNA glycosylase MutM. *Nat. Struct. Biol.* **9:** 544–552.

———. 2003. DNA lesion recognition by the bacterial repair enzyme MutM. *J. Biol. Chem.* **278:** 51543–51548.

Gilboa, R., Zharkov, D.O., Golan, G., Fernandes, A.S., Gerchman, S.E., Matz, E., Kycia, J.H., Grollman, A.P., and Shoham, G. 2002. Structure of formamidopyrimidine-DNA glycosylase covalently complexed to DNA. *J. Biol. Chem.* **277:** 19811–19816.

Jones, T., Zou, J-Y., Cowan, S.W., and Kjeldgaard, M. 1991. Improved methods for building protein models in electron density maps and the location of errors in these models. *Acta Crystallogr.* **A97:** 110–119.

Karplus, M. 2003. Molecular dynamics of biological macromolecules: A brief history and perspective. *Biopolymers* **68:** 350–358.

Lavrukhin, O.V. and Lloyd, R.S. 2000. Involvement of phylogenetically conserved acidic amino acid residues in catalysis by oxidative DNA damage enzyme formamidopyrimidine enzyme. *Biochemistry* **39:** 15266–15271.

Lindahl, T. 1993. Instability and decay of the primary structure of DNA. *Nature* **362:** 709–715.

Mackerell Jr., A.D., Bashford, D., Bellott, M., Dunbrack Jr., R.L., Evanseck, J.D., Field, M.J., Fischer, S., Gao, J., Guo, H., Ha, S., et al. 1998. All-atom empirical potential for molecular modeling and dynamics studies of proteins. *J. Phys. Chem. B* **102:** 3586–3616.

O'Connor, T.R. and Laval, J. 1989. Physical association of the 2,6-diamino-4-hydroxy-5N-formamidopyrimidine-DNA glycosylase of *Escherichia coli* and an activity nicking DNA at apurinic/apyrimidinic sites. *Proc. Natl. Acad. Sci.* **86:** 5222–5226.

Serre, L., Pereira, de Jésus K., Boiteux, S., Zelwer, C., and Castaing, B. 2002. Crystal structure of the *Lactococcus lactis* formamidopyrimidine-DNA glycosylase bound to an abasic site analogue-containing DNA. *EMBO J.* **21:** 2854–2865.

Sugahara, M., Mikawa, T., Kumasaka, T., Yamamoto, M., Kato, R., Fukuyama, K., Inoue, Y., and Kuramitsu, S. 2000. Crystal structure of a repair enzyme of oxidatively damaged DNA, MutM (Fpg), from an extreme thermophile, *Thermus thermophilus* HB8. *EMBO J.* **19:** 3857–3869.

Tchou, J., Kasai, H., Shibutani, S., Chung, M.H., Laval, J., Grollman, A.P., and Nishimura, S. 1991. 8-Oxoguanine (8-hydroxyguanine) DNA glycosylase and its substrate specificity. *Proc. Natl. Acad. Sci.* **88:** 4690–4696.

Vidal, A.E., Hickson, I.D., Boiteux, S., and Radicella, J.P. 2001. Mechanism of stimulation of the DNA glycosylase activity of hOgg1 by the major human AP endonuclease: Bypass of the AP lyase activity step. *Nucleic Acids Res.* **29:** 1285–1292.

Zaika, E.I., Perlow, R.A., Matz, E., Broyde, S., Gilboa, R., Grollman, A.P., and Zharkov, D.O. 2003. Substrate discrimination by formamidopyriminide-DNA glycosylase—A mutational analysis. *J. Biol. Chem.* **279:** 4849–4861.

Zharkov, D.O., Golan, G., Gilboa, R., Fernandes, A.S., Gerchman, S.E., Kycia, J.H., Rieger, R. A., Grollman, A.P., and Shoham, G. 2002. Structural analysis of an *Escherichia coli* endonuclease VIII covalent reaction intermediate. *EMBO J.* **21:** 789–800.